Article

Analogue Metric in a Black-Bounce Background

Kunal Pal, Kuntal Pal and Tapobrata Sarkar *

Department of Physics, Indian Institute of Technology Kanpur, Kanpur 208016, India; kunalpal@iitk.ac.in (K.P.); kuntal@iitk.ac.in (K.P.)
* Correspondence: tapo@iitk.ac.in

Abstract: The conventional approach of embedding an effective acoustic metric for sound motion in a background flat Minkowski space-time has recently been extended to incorporate more general curved background metrics, which might contain a black hole. Though the observational aspects of these kinds of acoustics horizons, including the sonic shadow structure and quasi normal modes, have received significant attention in the literature, there is room left for discussions about embedding more general classes of curved background space-times without optical horizons. Here, we propose and study a new class of acoustic metrics that is embedded in a black-bounce space-time, thereby giving a suitable tuneable system to understand possible observational effects of the presence or absence of acoustic horizons. After showing that the metric can represent five types of different effective backgrounds for sound motion, including a novel "acoustic wormhole–optical wormhole" branch, we discuss how the distinctive features of sonic shadows can appear even in the absence of any acoustic horizon due to the wormhole throat present in the acoustic metric.

1. Introduction

Einstein's general theory of relativity (GR) [1–4] remains the most successful theory of gravity to date and has been extensively tested at different scales. In this context, over the last four decades, there has been strong interest in studying various analogue models of gravity, as these can mimic gravitational phenomena in tabletop experiments. Indeed, after the pioneering work of Unruh [5] (for an excellent review, see [6]), there have been seminal works in the literature that focus on the experimental detection of gravitational effects via analogue gravity.

Analogue gravity is essentially based on the idea that dynamical equations of excitations in physical systems can often be mapped to ones in curved space-times. That is, these excitations "see" a curved space-time metric and this fact can then be used to obtain measurable effects in the laboratory that would then contain signatures of the metric itself. Physically, these would be reasonable as long as the analogue space-time is stable, a topic that has been much discussed in the literature. Given that experiments at astrophysical or cosmological scales present inherent difficulties, it is therefore natural that attempts at mimicking (i.e., engineering) appropriate curved space-times at such scales in the laboratory have been the focus of attention over the last many years. Although the theoretical idea of analogue gravity is almost four decades old, major experimental progress have happened only recently, and in the last decade, several such experiments have been reported, and promising results have been obtained. To date, such experiments have been performed, for example, in the context of fluids, optical systems, ultra-cold atoms, and so forth (for a sampling of the literature both on the theoretical and experimental aspects, see [7–20] and references therein. Some recent discussions on the validity and applicability of analogue models appear in [21,22]). With sophisticated technologies that can be used to carry out measurements with unprecedented accuracy rapidly becoming available, the hope is that analogue gravity experiments can be a tool for understanding deep aspects of the quantum

nature of gravity, such as the nature of the black hole event horizon, and related quantum fluctuations and entanglement.

Indeed, a significant number of studies on analogue gravity relate to black holes (BHs)—singular solutions of Einstein's equations that possibly hold the key to understanding strong gravity. Indeed, it is now believed that supermassive black holes exist in the central part of galaxies. The inherent importance of studying black holes lies in understanding one of the most intriguing unsolved questions regarding the fundamental nature of matter, namely that of quantum mechanics in the regime of strong gravity (in other words, quantum gravity). Against this backdrop, it is natural that a large amount of existing literature seeks to understand so called "acoustic" black holes, a background formed, for example, with moving fluids with the "event horizon" in such backgrounds being the location of the fluid where its speed exceeds that of sound.

In a recent work, Ref. [23] extended the above line of work and showed how to embed analogue acoustic black holes in a curved background. This is in contrast to the models studied earlier where analogue black holes were constructed in Minkowski space-time. In such a background, an excited state of a fluid will "see" a more general acoustic metric than that of its flat space-time counterpart. This is important and interesting for two reasons. First, although often idealised by vacuum solutions of Einstein's equations, the backgrounds of astrophysical black holes are possible fluid systems that may arise due to effects such as accretion after tidal disruption processes. Hence it is more realistic to model analog astrophysical black holes in terms of fluids with a background curvature. Secondly, the extra freedom present with such curved backgrounds offer the interesting possibility of constructing exotic solutions that can possibly be mimicked in the laboratory.

On the other hand, among the most intriguing observational aspects of ultracompact objects such as black holes, wormholes (WHs), naked singularities and so forth, which can bend light to form a photon ring, is the shadow of the given spacetime of interest. This research direction has seen a flurry of interest especially in the wake of the recent observation of the shadow of the supermassive object at the centre of our galaxy by the event horizon telescope [24,25]. It is not hard to believe that such studies can also shed light on many important aspects of analogue gravity models and the respective acoustic metrics. In this regard, several works appear in the literature (see e.g., [26,27]) where the sonic shadow of the acoustic metric in a curved background is studied. On the other hand, in a real life laboratory setup, mimicking the actual light bending for sound waves in the presence of acoustic horizons can be problematic, mainly due to the fact that the acoustic horizon can be dynamically unstable due to the effect of the Hawking radiation present in the system (for extensive discussions see [6] and references therein). Hence, studying a system which can still offer the analogous effect of strong light bending even in the absence of the acoustic horizon is important, and understanding the differences of this, with that of conventional acoustic black holes can offer valuable insights regarding fundamental aspects of analogue gravity.

In view of the above discussions, here we will take the background to be the recently constructed black bounce space-time of Simpson and Visser (SV) [28]. The SV solution is a one-parameter family of space-times that interpolates between a deformed Schwarzschild black hole and a traversable wormhole of the Morris–Thorne class. Using this as the background, here we construct an acoustic metric that can represent (1) a WH–WH system; (2) a BH–WH system; and (3) a BH–BH system with single and double horizons, depending on the SV parameter and the acoustic parameter that specifies the escape velocity from the background metric. In particular, we show that there are two extremely interesting possibilities that may arise. First, one can have sonic rings even in the absence of an acoustic event horizon. As already stated, this fact assumes importance given that such acoustic horizons may generically be dynamically unstable. Second, we show here that the acoustic SV background indicates that we can in principle distinguish between a WH–WH system and a BH–WH system by taking advantages of some of the novel features of null geodesic motion in wormhole backgrounds.

This paper is organised as follows. Section 2 briefly reviews the necessary background material. In Section 3, we construct the acoustic metric, whose structure is analysed in Section 4, where various ranges of parameters are considered. Section 5 deals with observational aspects of the solution, and we conclude with some discussions in Section 6.

2. Acoustic Metric in Curved Background

In this section we briefly review the construction of the acoustic metric from the Gross–Pitaevskii (GP) theory following [23]. We consider the propagation of a complex scalar field ($\Phi(x^\mu)$) obeying the Gross–Pitaevskii equation on a static background metric of the form:

$$ds_{bg}^2 = g_{tt}(r)\mathrm{d}t^2 + g_{rr}(r)\mathrm{d}r^2 + r^2(\mathrm{d}\theta^2 + \sin^2\theta\mathrm{d}\phi^2) \,. \tag{1}$$

Substituting $\Phi(x^\mu) = \sqrt{\rho(x^\mu)}e^{\Theta(x^\mu)}$ in the GP equation, then considering a perturbation around the background fields Θ_0, ρ_0 and furthermore working in the long wavelength limit, Ref. [23] derived a general form of the effective metric. The general form of the acoustic metric is complicated and is in general not diagonal. Here, since we want to find out the acoustic geometry corresponding to the SV spacetime, it is sufficient to consider a simpler background static metric such that $g_{rr}(r)g_{tt}(r) = -1$, and we will also assume that the θ, ϕ components of the background four-velocity vanishes, that is, $v_\theta = v_\phi = 0$. In that case, it is possible to render the acoustic metric in a convenient diagonal form, by making a change of the time coordinate as:

$$\mathrm{d}t = \mathrm{d}\tilde{t} + \frac{v_t v_r}{g_{tt}\left(c_s^2 - v_r v^r\right)}\mathrm{d}r \,, \tag{2}$$

where c_s is the speed of sound and v_μ is the four-velocity of the fluid. c_s can be obtained by knowing the background value of the modulus of the complex scalar field, and by specifying the constants appearing in the GP theory. The phase of the complex scalar field determines the components of the four-velocity by the relations $v_t = -\partial_t\Theta_0$ and $v_i = -\partial_i\Theta_0$ with $i = r, \theta, \phi$. The conditions $v_\theta = 0$ and $v_\phi = 0$ mean that the background phase Θ_0 is independent of the angular coordinates θ, ϕ. Furthermore, we shall work in the critical temperature of the GP theory so that the normalisation condition satisfied by the background four-velocity of the fluid is $v_\mu v^\mu = -2c_s^2$.

Following all the above steps, the acoustic metric derived in terms of the coordinates $\tilde{t}, r, \theta, \phi$ is given by [23]

$$ds_{ac}^2 = c_s\sqrt{c_s^2 - v_\mu v^\mu}\left[\frac{c_s^2 - v_r v^r}{c_s^2 - v_\mu v^\mu}g_{tt}\mathrm{d}\tilde{t}^2 + \frac{c_s^2}{c_s^2 - v_r v^r}g_{rr}\mathrm{d}r^2 + r^2\left(\mathrm{d}\theta^2 + \sin^2\theta\mathrm{d}\phi^2\right)\right] \,. \tag{3}$$

Here the time coordinates $\tilde{t}$ appearing in the acoustic line element ds_{ac}^2 is different from the time coordinate t appearing in the background line element.

Now we re-scale the velocity vector as $v_\mu v^\mu = 2c_s^2\tilde{v}_\mu\tilde{v}^\mu$, such that the new one satisfies the usual normalisation condition $\tilde{v}_\mu\tilde{v}^\mu = -1$. Substituting this in the acoustic line element, and removing all the tildes for notational convenience, and further denoting $g_{tt}(r) = f(r) = g_{rr}(r)^{-1}$, we obtain the following form for the acoustic metric:

$$ds_{ac}^2 = \sqrt{3}c_s^2\left[(1 - 2v_r v^r)f(r)\mathrm{d}t^2 + \frac{1}{f(r)\left(1 - 2v_r v^r\right)}\mathrm{d}r^2 + r^2\left(\mathrm{d}\theta^2 + \sin^2\theta\mathrm{d}\phi^2\right)\right] \,. \tag{4}$$

From now on, we will put $\sqrt{3}c_s^2 = 1$. Given a static background metric of the form in Equation (1) obeying $g_{rr}(r)g_{tt}(r) = -1$, that is, with a specified functional form of $f(r)$ we can easily obtain the corresponding acoustic metric using Equation (4). This form of acoustic metric has attracted a lot of recent attention due to its simple analytical form and potential experimental applications, and has been explored recently in [26–33]. Notably, most of the above cited recent works explore the acoustic metric in black hole backgrounds,

with stationary and slowly rotating versions considered in [29]. This leads to the natural question of whether we can generalise these metrics for more generic backgrounds, such as wormhole geometries or non singular geometries, and if so, what special features those acoustic metrics might show.

This is what we set out to do in the next sections and our aim will be to construct the corresponding acoustic metric and study its properties, when the background is the recently proposed one parameter generalisation of the Schwarzschild metric, namely the SV [28] geometry.

3. Acoustic Metric in the Black-Bounce Background

As a background metric we choose to work with the black-bounce space-time introduced by SV, which can represent a regular black hole (BH) or a (one-way or two-way) traversable wormhole (WH), depending on the parameter range of interest. The SV solution is given by:

$$ds_{bc}^2 = -\left(1 - \frac{2M}{\sqrt{r^2 + \beta^2}}\right)dt^2 + \left(1 - \frac{2M}{\sqrt{r^2 + \beta^2}}\right)^{-1}dr^2 + \left(r^2 + \beta^2\right)d\Omega^2 . \tag{5}$$

Here, $\beta > 0$ is a constant and the range of the r coordinate is $-\infty$ to ∞. For different values of β (in comparison to the mass M), the above metric may represent the following: (1) For $\beta > 2M$, the SV metric represents a two-way traversable wormhole; (2) when $\beta = 2M$, it describes a one-way wormhole, and finally; (3) for $\beta < 2M$ it is a regular black hole. The introduction of the non zero constant β helps to remove the central singularity of the Schwarzschild space-time. In the last case, the regular black hole has two horizons at the locations $r_{\pm} = \pm\sqrt{(2M)^2 - \beta^2}$.

Let us now consider the motion of a relativistic fluid moving in this background. Following [26], we consider the radial velocity of the fluid to be of the form $v_r = \sqrt{\frac{2M}{\sqrt{r^2 + \beta^2}}}\xi$ such that the fluid is not trapped by the background geometry. This can be ensured by choosing the radial velocity to be greater than the escape velocity, that is, by taking the factor $\xi \geq 1$. As mentioned before, working in the critical temperature regime of Gross–Pitaevskii theory, and after the rescaling of the four velocity, we arrive at the following acoustic metric as "seen" by sonic excitations:

$$ds_{ac}^2 = \sqrt{3}c_s^2\left[-F(r)dt^2 + G(r)^{-1}dr^2 + \left(r^2 + \beta^2\right)d\Omega^2\right] , \tag{6}$$

where we have defined

$$F(r) = G(r) = \left(1 - \frac{2M}{\sqrt{r^2 + \beta^2}}\right)\left[1 - \frac{2M\xi}{\sqrt{r^2 + \beta^2}}\left(1 - \frac{2M}{\sqrt{r^2 + \beta^2}}\right)\right] . \tag{7}$$

It is easy to check that this metric possesses all the well defined limits that have appeared in the literature, namely in the limit $\xi \to 0$, it reduces to the original back ground SV metric. On the other hand, in the limit $\beta \to 0$, it gives us the acoustic metric in the Schwarzschild background discussed recently in [27].

4. Structure of the Acoustic Metric

In this section, we discuss details the nature of the objects that the acoustic metric can represent, depending on the different ranges of the parameter values involved. To analyse this more clearly, we perform a simple coordinate transformation $r^2 + \beta^2 = k^2$, such that the area of the two sphere part is now given by $4\pi k^2$. The (radial) g_{kk} term now reads:

$$g_{kk} = \frac{k^2}{(k^2 - \beta^2)\left(1 - \frac{2M}{k}\right)\left(1 - \frac{2M\xi}{k}\left(1 - \frac{2M}{k}\right)\right)} . \tag{8}$$

The last factor in the denominator of g_{kk} gives the polynomial $k^2 - 2M\xi k + 4M\xi^2$, and hence it can be seen that the denominator has four positive roots and their interplay will determine the nature of the acoustic metric. The four roots are:

$$k_1 = \beta, \quad k_2 = 2M, \quad \text{and} \quad k_{3,4} = M\xi \mp M\sqrt{\xi^2 - 4\xi}. \tag{9}$$

In comparison with the original SV metric (when written in the k coordinate), we can see that the first two roots k_1, k_2 have their origin in the background SV metric, whereas the novel contribution of the fluid velocity in the acoustic metric (through the parameter ξ) is manifested in the last two solutions k_3, k_4. In order to make these roots real, we can see that the allowed range of parameter ξ has to be $\xi \geq 4$ and for $\xi = 4$, these two roots coincide, making the solution extremal. Note that when k_3, k_4 are real, they are always greater than k_2.

Considering the motion of a null particle ($ds^2 = 0$), we have:

$$\frac{dr}{dt} = F(r) = \left(1 - \frac{2M}{\sqrt{r^2 + \beta^2}}\right)\left[1 - \frac{2M\xi}{\sqrt{r^2 + \beta^2}}\left(1 - \frac{2M}{\sqrt{r^2 + \beta^2}}\right)\right]. \tag{10}$$

From this light-cone structure, we can infer different cases depending on the values of β. The solution of the equations:

$$1 - \frac{2M}{\sqrt{r^2 + \beta^2}} = 0, \quad 1 - \frac{2M\xi}{\sqrt{r^2 + \beta^2}}\left(1 - \frac{2M}{\sqrt{r^2 + \beta^2}}\right) = 0, \tag{11}$$

will give rise to none, one or many horizons, as these are the positions where the light cones flip. For later purposes, we note the solutions to be (only those are positive for the parameter ranges and hence on "our side" of the universe):

$$r_1 = \sqrt{4M^2 - \beta^2}, \quad r_2 = \sqrt{2\left(M^2(\xi - 2)\xi - \sqrt{M^4(\xi - 4)\xi^3}\right) - \beta^2},$$

$$\text{and} \quad r_3 = \sqrt{2\left(\sqrt{M^4(\xi - 4)\xi^3} + M^2(\xi - 2)\xi\right) - \beta^2}. \tag{12}$$

If we take $\xi \geq 4$, then both the solutions r_3 and r_2 are greater than r_1. The optimal ranges of β upon which the structure of the metric depends can be easily obtained by solving Equation (11) for $r = 0$, which are identical to those of k_2, k_3, k_4.

4.1. Case 1: $\beta > k_4, \xi \geq 4$: Acoustic Wormhole, Optical Wormhole

In this parameter range, for sound waves, the metric behaves like a two way traversable wormhole with a throat at $r = 0$, and for light rays (which move in the background metric), the system behaves like a wormhole. We will call this a WH–WH system. This can be seen from Equation (10), that since $\frac{dr}{dt}$ is never zero with this range of parameters, the absence of a horizon in the acoustic metric is guaranteed. It can also be seen that, in this case, the acoustic metric consists of two copies of the same metric glued at $k = \beta$ (in the original coordinates this location is at $r = 0$) since the metric can be extended from $r = -\infty$ to $r = 0$ to $r = \infty$. [1] The traversability can be confirmed by checking the so called 'flaring out' condition for a wormhole, which ensures that the throat is the location of the minimum area, and establishes the absence of a horizon in this space-time [35]. Mathematically, this demands that at the throat $\mathbf{R}'(r = r_0) = 0, \mathbf{R}''(r = r_0) > 0$ with $\mathbf{R}(r)$ being the two sphere part of the metric. It is also crucial to check that the geometry is non singular everywhere, which can be confirmed by calculating the Ricci and the Kretschmann scalar. The Ricci scalar corresponding to the metric in Equation (6) is:

$$\mathbf{R}(r) = \frac{1}{(r^2 + \beta^2)^{7/2}} \left[16M^3 r^2 \xi + \beta^4 \left(6M(1 + \xi) - 2\sqrt{r^2 + \beta^2} \right) + \beta^2 \left(6Mr^2(1 + \xi) + 8M^3 \xi \right. \right.$$
$$\left. \left. - 16M^2 \sqrt{r^2 + \beta^2} - 2r^2 \sqrt{r^2 + \beta^2} \right) \right].$$

(13)

It can be easily checked that as $r \to 0$, the Ricci scalar takes a constant value. A similar conclusion is valid for the Kretschmann scalar as well.

This particular branch of the acoustic metric offers novel features of sound motion which, to the best of our knowledge, have not appeared in the literature before. As we shall describe below, here we can observe the strong bending of sound and consequently sonic rings even in the absence of any acoustic event horizon—which is a specialty of photon motion in a wormhole background. In view of the generic dynamical instability of the acoustic event horizons [6], this regular WH–WH system can offer an interesting 'stable' system to experimentally observe the related observational signatures. As a caveat, we add that, admittedly, the construction of wormholes in general relativity require so-called 'exotic matters' that might violate the standard energy conditions, but these can be realised in many modified gravity setups with regular matter sources.

4.2. Case 2: $k_3 < \beta < k_4, \xi \geq 4$: Acoustic Black Hole (One Horizon), Optical Wormhole

This is another interesting situation, where the metric possesses an outer acoustic horizon at $r = r_3$ so that the acoustic metric describes an acoustic black hole with a space-like throat (though this term should not be strictly used for sound waves) at $r = 0$ that is only one way traversable (due to the presence of the horizon). This is seen from the fact that the light cone flips at $r = r_3$. Crucially, in this case, the space-time metric is still a wormhole (two way traversable) with a time-like throat at $k = \beta$ ($r = 0$) since, by the imposed conditions above, $\beta > k_2$ is always satisfied. We call this a BH–WH system.

Here, the appearance of the acoustic horizon in the absence of any background event horizon signifies the fact that the sound cone can flip even though the light cone does not. Hence, every optical horizon is an acoustic horizon but the reverse is not true. This type of regular acoustic geometry (BH–WH system) is also a novel addition to the existing literature, and offers a different sonic shadow structure to that of the WH–WH system of case 1, depending on the source of sound present. It is well known that if the source is present on the other side of the throat compared to the observer, the wormhole can cast qualitatively different shadows than that of a black hole. In an entirely similar way, here we can in principle distinguish the two different systems (WH–WH and BH–WH) by observing their corresponding sonic rings.

4.3. Case 3: $k_2 < \beta < k_3(< k_4), \xi \geq 4$: Acoustic Black Hole (Two Horizons), Optical Wormhole

In this case, the metric possesses both inner and outer horizons at r_3, and r_2, since both of them are real when the above restrictions are imposed. Thus, the acoustic metric represents a multi-horizon acoustic black hole with a time-like throat at $r = 0$. This is in contrast with case 2 above, where the throat was space-like. But again (like case 2) the optical geometry is a two way traversable wormhole since the condition $\beta > k_2$ is still satisfied here.

4.4. Case 4: $\beta < k_2, \xi \geq 4$: Acoustic Black Hole, Optical Black Hole

Here, β is less than k_2, hence the acoustic metric is a acoustic black hole with three horizons (one coming from the original background metric and the other two are acoustic horizons). The background is also a regular black hole with a single horizon at $k = 2M$ with a space-like throat at $r = 0$. This case is qualitatively similar to the one reported in [23,26], where the background geometry was taken to be the Schwarzschild solution.

4.5. Case 5: $\xi < 4$ Acoustic and Optical Geometry Qualitatively Same

Finally, in this case none of the solutions r_2, r_3 are real and the acoustic metric has the same structure as that of the background SV metric (though they have different coordinate dependence), and will represent a black hole or traversable wormhole depending on the values of the SV parameter β.

5. Observational Aspects of the Black-Bounce Acoustic Metric

One of the most studied aspects of a space-time metric containing a black hole or a wormhole is its shadow structure, which is defined as the region of the observer's sky which is left dark. This aspect of BHs and WHs is extremely well studied in the literature, and its importance has increased significantly after the recent observation of the shadow of the compact object at the centre our galaxy by the Event Horizon Telescope. In the traditional study of the shadow of a compact object (with or without a horizon), an important aspect is the behaviour of null geodesics, which can lead to interesting phenomena, such as the formation of Einstein rings.

For the spherically symmetric and static metrics that we have considered, the study of null geodesics is simple, due to the presence of integrals of motions, and hence can be treated analytically. Here our main goal will be to study the observational aspects of the acoustic metric in black-bounce space-times derived above by the standard assumption that the sound waves move in null geodesics in this acoustic metric. This is in the same sense as light waves moving in a space-time metric, such that the standard approach to solving this problem involving the effective potential (encountered by a photon) can be implemented. In particular, our emphasis will be on the availability and the study of the analogue of the 'photon sphere' or the 'anti-photon sphere', which are the unstable (or stable) circular orbits of photons (here sound waves) that may give rise to *acoustic shadow* for some listener far away from the acoustic black hole (or wormhole).

The conventional analytical approach to study the motion of the null geodesics is to employ the Hamilton–Jacobi equation given by:

$$\frac{\partial S}{\partial \lambda} + H = 0 \, , \; H = \frac{1}{2} g_{\mu\nu} p^\mu p^\nu \, . \tag{14}$$

Here, H is the Hamiltonian of the particle, S is the Jacobi action, λ is an affine parameter that parametrises a geodesic, and p^μ is the 4-momentum vector defined by $p_\mu = \frac{\partial S}{\partial x^\mu}$. Since the acoustic metric is static and spherically symmetric, there are two constants of motion associated with the particle motion, namely the energy $E = -p_t$ and the angular momentum $L = -p_\phi$. Then, assuming a separable form of the Jacobi action, we can write down the effective potential for the motion of the null rays in the radial direction to be [36]

$$V_{eff}(r) = \mathcal{G}_{tt} \frac{L^2}{\mathbf{R}(r)} \, , \tag{15}$$

where $\mathcal{G}_{tt}$ is the temporal component of the acoustic metric, and $\mathbf{R}(r)$ is its two sphere part. Now the *photon sphere* (or the *anti-photon sphere*), which determines the boundary of the shadow is given by the extrema of the effective potential, and our study in this case reduces to analysing the resulting effective potential for this metric.

Substituting $\mathcal{G}_{tt}$ from Equation (7) in Equation (15) we have the expression for the effective potential to be:

$$V_{eff}(r) = \frac{L^2}{\beta^2 + r^2} \left(1 - \frac{2M}{\sqrt{\beta^2 + r^2}} \right) \left(1 - \frac{2M\xi \left(1 - \frac{2M}{\sqrt{\beta^2 + r^2}} \right)}{\sqrt{\beta^2 + r^2}} \right) . \tag{16}$$

Now imposing the condition $V'_{eff}(r) = 0$, we can read off the extrema of the effective potential. In this case, these are given by the solutions of the equation:

$$r^2\sqrt{\beta^2 + r^2} - 20M^3\xi + 16M^2\xi\sqrt{\beta^2 + r^2} - 3M(\xi + 1)r^2 + \beta^2\left(\sqrt{\beta^2 + r^2} - 3M(\xi + 1)\right) = 0\,. \tag{17}$$

A trivial solution is at $r = 0$, which will be of interest later in the wormhole case. The analytical expressions for the other solutions of this equation are complicated, and we will not write them here for brevity. Rather, we plot the effective potential to directly obtain the corresponding locations of the maxima (corresponding to the unstable photon orbits, i.e., the photon sphere) and minima (stable photon orbits, i.e., the anti-photon sphere) for given values of the parameters. It is important to note that, when the acoustic metric represents a WH, apart from the photon spheres that are outside the throat (solution of Equation (17) with maximum of the effective potential), the throat itself can act as a location of the unstable light rays, and hence can give rise to an additional photon sphere. For details of this and related issues see [37]. Now, we shall consider the different cases that can appear.

5.1. Case-1: Acoustic Wormhole ($\beta > k_4, \xi \geq 4$)

In this case, the metric represents an acoustic wormhole, and the condition $\beta > k_4$ imposes a restriction on the possible values that the SV parameter can take in this range, which in turn gives two types of effective potentials. Below we discuss different possible scenarios depending on the value of β for a particular choice of M and ξ, taken for the purpose of illustration as $M = 1, \xi = 4.1$. From Equation (17), we see that for these values of the parameters, this equation can have either one positive real solution or no real root at all.

5.1.1. Case 1.1: One Photon Sphere per Side

For the choice of parameters $M = 1, \xi = 4.1$ and $L = 1$, we find that $k_4 = 4.74$, so we are restricted to take the value of β to be above this limit. As can be directly seen from the plot of the effective potential shown in Figure 1, for values of $\beta > k_4 = 4.74$, up to a critical value, the null rays encounter only one photon sphere per side of the throat. Note that the numerical choices made here are for illustration only. For example, for different values of L, the profile of the effective potential remains qualitatively the same, and only its magnitude is changed.
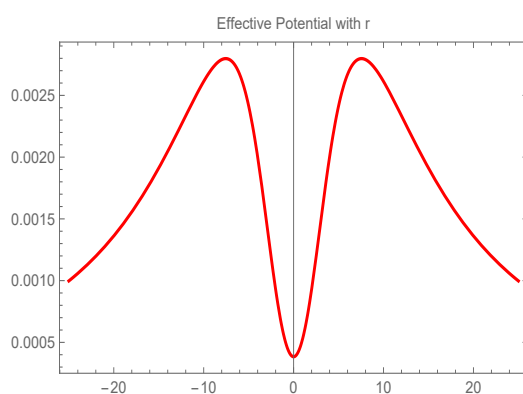

Figure 1. Variation of the effective potential with r for $\beta = 5$, $M = 1$, $L = 1$, and $\xi = 4.1$.

5.1.2. Case 1.2: No Photon Sphere outside the Throat

If the value of the SV parameter β goes above a certain limit, we observe an interesting feature of the effective potential that is typical of many wormhole solutions. Here, none of the roots of Equation (17) are real, and instead the effective potential is at a maximum at $r = 0$ indicating that the throat itself is a location of the unstable photon orbits. We have shown this case for $\beta = 9.5$ for $M = 1, \xi = 4.1$ and $L = 1$ in Figure 2.
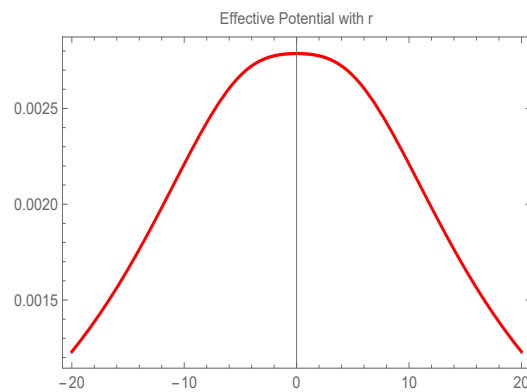
Figure 2. Variation of the effective potential with r for $\beta = 9.5$, $M = 1$, $L = 1$, and $\xi = 4.1$.

In both these cases, the sonic ring is formed in an acoustic wormhole metric where the acoustic horizon is absent. This is a special feature of many wormhole metrics. Note, however, that though the above two cases represent WH–WH systems, the strong bending formula and associated observables are different for case (1.1) and case (1.2), which indicates an important distinction between these two cases (see [38] for details).

5.2. Case 2: Single Horizon Acoustic Black Hole ($k_3 < \beta < k_4, \xi \geq 4$)

In this case, as the metric represents an acoustic black hole with a single horizon, the profile of the effective potential and the structure of the related photon spheres are standard, and are discussed in the literature widely. We will not go into the details here, and only present a plot of the effective potential in Figure 3 for completeness. Note again that the strong bending observables are also different from that of the above cases (1.1), (1.2) and in principle can serve as an important distinguishing feature between these two classes of geometries.

Similar scenarios occur for case-3 and case-4 of the previous section even though multiple horizons are present in these cases.
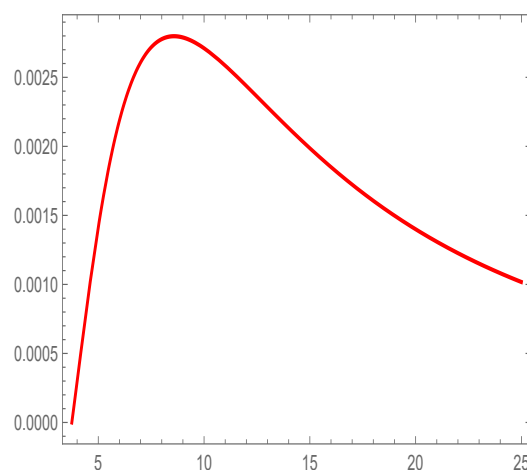

Figure 3. Variation of the effective potential with r for $\beta = 2.9$ for $M = 1$, $L = 1$ and $\xi = 4.1$.

Finally, we consider the shadow contour in our acoustic metric. The shadow of a typical black hole (or any compact object) for a faraway observer consists of the projection of the photon sphere to the observer's plane. For a non rotating metric, this reduces to finding two celestial coordinates X, Y that describe the outline of the shadow by following the constraint relation $X^2 + Y^2 = r_{sh}^2$, where r_{sh} is the shadow radius, which for an observer at infinity can be written down as $r_{sh} = \sqrt{\left.\frac{\mathbf{R}(r)^2}{G_{tt}}\right|_{r=r_{ph}}}$. For our acoustic metric, in an entirely

similar manner, we can define the shadow for motion of sound waves, which is a region for a "listener at infinity" that will be void of any sound.

In Figure 4, we have plotted the shadow contour for various parametric values. Interestingly, the shadow radius increases with ξ, which characterises the medium in which the sound is propagating. We can see that an increasing area of the listener's plane will be soundless with increasing ξ. In this figure, we have drawn the shadow contours for a value of β in the wormhole branch for different values of ξ.
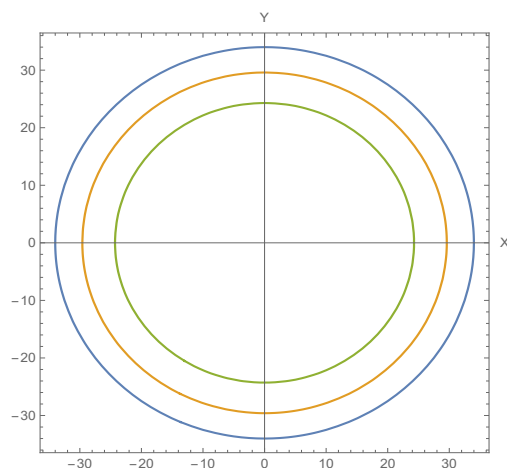

Figure 4. Plot of the shadow contour with varying ξ, with $\beta = 12$ and $M = 1$. The blue curve has $\xi = 7.1$, the yellow $\xi = 6.1$ and the green has $\xi = 5.1$.

6. Conclusions

The traditional construction of the acoustic metrics for sound motion in a fluid with a flat background (Minkowski space-time) has recently been extended to include more general curved background space-time metrics. This opens up a new and interesting direction to study sound motion in a realistic black hole (or compact object) background immersed in some fluid. In this paper, we have taken a step further in this direction to take a general background metric into consideration, namely the recently proposed Simpson–Visser black-bounce metric, which interpolates between a regular black hole and a wormhole for different values of a single parameter.

Considering sound motion in a fluid in this geometry, we have elucidated the resulting acoustic metric in detail. We have shown that the acoustic horizon may or may not be present even in the absence of the optical event horizon depending on the interplay between the parameters in question. As a result, sound can be trapped (from the outside observer) in two ways; the first one is due solely to the acoustic horizon present in the geometry, and the second one is due to the optical event horizon itself, as the optical event horizon is also an acoustic horizon. The converse is however not true, and as a result we cannot have an acoustic wormhole in a black hole background. In summary, we have constructed a novel acoustic metric, which, depending on the parameter region, can broadly represent: (1) an acoustic wormhole and optical wormhole (WH–WH) geometry; (2) acoustic black hole (with a single horizon or multiple horizons) and optical wormhole (BH–WH) geometry; (3) acoustic black hole and optical black hole (BH–BH) geometry. This can be of importance from an experimental point of view, where the acoustic horizon, in the absence of an optical horizon, may be easier to simulate.

To elucidate the observational signatures of this metric, and to contrast how this family is different from those that have appeared in the literature (all of these are in black hole background, i.e., in our notation, of the BH–BH type), we have explored one of the standard ways to distinguish a BH from a WH, namely the shadow structure of the given metric. The special feature for light motion shown by most wormhole metrics is the presence of a photon ring (and sphere) due to light bending at the throat itself—the sonic analogy of this fact is used here to show how a similar feature for sound can produce a *sonic ring*

due to the acoustic wormhole throat, in addition to the known sonic rings due to the acoustic horizons. As a result, sonic rings can still be produced even in the absence of any acoustic horizons, which can have potential experimental realisation. In this paper, we have taken a spherically symmetric background to describe the acoustic metric. Slowly rotating backgrounds have been recently discussed in the work of [29], and a generalisation of our results to rotating backgrounds and the observational signature of these should be an important direction for future work.

Author Contributions: Conceptualization, K.P. (Kunal Pal), K.P. (Kuntal Pal), T.S.; methodology, K.P. (Kunal Pal), K.P. (Kuntal Pal); formal analysis, K.P. (Kunal Pal), K.P. (Kuntal Pal); investigation, K.P. (Kunal Pal), K.P. (Kuntal Pal); writing—original draft preparation, K.P. (Kunal Pal), K.P. (Kuntal Pal); writing—review and editing, K.P. (Kunal Pal), K.P. (Kuntal Pal), T.S. All authors have read and agreed to the published version of the manuscript.

Institutional Review Board Statement: Not applicable.

Informed Consent Statement: Not applicable.

Conflicts of Interest: The authors declare no conflict of interest.

Note

1　In an experimental setup, we cannot have an acoustic wormhole that connects two asymptotically flat space-times, but here we are only interested in "our side" of the wormhole, where the acoustic analogue of the WH throat may leave its imprint. See [34] for a detailed discussion.

References

1.　Weinberg, S. *Gravitation and Cosmology*; John Wiley and Sons: New York, NY, USA, 1972.
2.　Wald, R.M. *General Relativity*; University of Chicago Press: Chicago, IL, USA, 2010.
3.　Hartle, J.B. *Gravity: An Introduction to Einstein's General Relativity*; AAPT: North Sydney, Australia, 2003.
4.　Poisson, E. *A Relativist's Toolkit, the Mathematics of Black-Hole Mechanics*; Cambridge University Press: Chicago, IL, USA, 2004.
5.　Unruh, W.G. Experimental black-hole evaporation? *Phys. Rev. Lett.* **1981**, *46*, 1351. [CrossRef]
6.　Barcelo, C.; Liberati, S.; Visser, M. Analogue gravity. *Living Rev. Relativ.* **2005**, *8*, 12. [CrossRef] [PubMed]
7.　Visser, M. Acoustic propagation in fluids: An Unexpected example of Lorentzian geometry. *arXiv* **1993**, arXiv:9311028.
8.　Visser, M.; Weinfurtner, S.E.C. Vortex geometry for the equatorial slice of the Kerr black hole. *Class. Quant. Grav.* **2005**, *22*, 2493. [CrossRef]
9.　Barcelo, C.; Liberati, S.; Sonego, S.; Visser, M. Causal structure of acoustic space-times. *New J. Phys.* **2004**, *6*, 186. [CrossRef]
10.　Rousseaux, G.; Mathis, C.; Maissa, P.; Philbin, T.; Leonhardt, U. Observation of negative-frequency waves in a water tank: A classical analogue to the Hawking effect. *New J. Phys.* **2008**, *10*, 053015. [CrossRef]
11.　Philbin, T.; Kuklewicz, C.; Robertson, S.; Hill, S.; Konig, F.; Leonhardt, U. Fiber-Optical Analog of the Event Horizon. *Science* **2008**, *319*, 1367. [CrossRef]
12.　Belgiorno, F.; Cacciatori, S.; Clerici, M.; Gorini, V.; Ortenzi, G.; Rizzi, L.; Rubino, E.; Sala, V.; Faccio, D. Hawking Radiation from Ultrashort Laser Pulse Filaments. *Phys. Rev. Lett.* **2010**, *105*, 203901. [CrossRef]
13.　Weinfurtner, S.; Tedford, E.; Penrice, M.; Unruh, W.; Lawrence, G. Measurement of Stimulated Hawking Emission in an Analogue System. *Phys. Rev. Lett.* **2011**, *106*, 021302. [CrossRef]
14.　Lahav, O.; Itah, A.; Blumkin, A.; Gordon, C.; Rinott, S.; Zayats, A.; Steinhauer, J. Realization of a Sonic Black Hole Analog in a Bose-Einstein Condensate. *Phys. Rev. Lett.* **2010**, *105*, 240401. [CrossRef]
15.　Hossenfelder, S. Analog systems for gravity duals. *Phys. Rev. D* **2015**, *91*, 124064. [CrossRef]
16.　Shammass, I.; Rinott, S.; Berkovitz, A.; Schley, R.; Steinhauer, J. Phonon Dispersion Relation of an Atomic Bose-Einstein Condensate. *Phys. Rev. Lett.* **2012**, *109*, 195301. [CrossRef] [PubMed]
17.　Schley, R.; Berkovitz, A.; Rinott, S.; Shammass, I.; Blumkin, A.; Steinhauer, J. Planck distribution of phonons in a Bose-Einstein condensate. *Phys. Rev. Lett.* **2013**, *111*, 055301. [CrossRef]
18.　Steinhauer, J. Observation of self-amplifying Hawking radiation in an analogue black-hole laser. *Nat. Phys.* **2014**, *10*, 864. [CrossRef]
19.　Steinhauer, J. Observation of quantum Hawking radiation and its entanglement in an analogue black hole. *Nat. Phys.* **2016**, *12*, 959. [CrossRef]
20.　Ge, X.H.; Sin, S.J. Acoustic black holes for relativistic fluids. *JHEP* **2010**, *6*, 087. [CrossRef]
21.　Crowther, K.; Linnemann, N.; Wuthrich, C. What we cannot learn from analogue experiments. *Synthese* **2021**, *198*, 3701. [CrossRef]
22.　Barcelo, C.; Garay, L.; Garcia-Moreno, G. Superposing spacetimes: Lessons from analogue gravity. *arXiv* **2021**, arXiv:2104.15078.

23. Ge, X.-H.; Nakahara, M.; Sin, S.-J.; Tian, Y.; Wu, S.-F. Acoustic black holes in curved spacetime and the emergence of analogue Minkowski spacetime. *Phys. Rev. D* **2019**, *99*, 104047. [CrossRef]
24. The Event Horizon Telescope Collaboration. First M87 Event Horizon Telescope Results. I. The Shadow of the Supermassive Black Hole. *Astrophys. J. Lett.* **2019**, *875*, L1. [CrossRef]
25. The Event Horizon Telescope Collaboration. First M87 Event Horizon Telescope Results. VI. The Shadow and Mass of the Central Black Hole. *Astrophys. J. Lett.* **2019**, *875*, L6. [CrossRef]
26. Ling, R.; Guo, H.; Liu, H.; Kuang, X.M.; Wang, B. Shadow and near-horizon characteristics of the acoustic charged black hole in curved space-time. *Phys. Rev. D* **2021**, *104*, 104003. [CrossRef]
27. Guo, H.; Liu, H.; Kuang, X.H.; Wang, B. Acoustic black hole in Schwarzschild space-time: Quasi-normal modes, analogous Hawking radiation and shadows. *Phys. Rev. D* **2020**, *102*, 124019. [CrossRef]
28. Simpson, A.; Visser, M. Black-bounce to traversable wormhole. *J. Cosmol. Astropart. Phys.* **2019**, *2*, 042. [CrossRef]
29. Vieira, H.S.; Destounis, K.; Kokkotas, K.D. Slowly-rotating curved acoustic black holes: Quasinormal modes, Hawking-Unruh radiation and quasibound states. *arXiv* **2021**, arXiv:2112.08711 .
30. Anacleto, M.A.; Brito, F.A.; Luna, G.C.; Passos, E. The generalized uncertainty principle effect in acoustic black holes. *arXiv* **2021**, arXiv:2112.13573.
31. Lan, C.; Miao, Y.G.; Zang, Y.X. Acoustic regular black hole in fluid and its similarity and diversity to a conformally related black hole. *arXiv* **2021**, arXiv:2109.13556.
32. Qiao, C.K.; Zhou, M. The Gravitational Bending of Acoustic Schwarzschild Black Hole. *arXiv* **2021**, arXiv:2109.05828.
33. Yuan, H.; Ge, X.H. Analogue of the pole-skipping phenomenon in acoustic black holes. *arXiv* **2021**, arXiv:2110.08074.
34. Nandi, K.K.; Zhang, Y.Z.; Cai, R.G. Acoustic wormholes. *arXiv* **2004**, arXiv:0409085 .
35. Simpson, A. Traversable Wormholes, Regular Black Holes, and Black-Bounces. *arXiv* **2021**, arXiv:2104.14055.
36. Sau, S.; Banerjee, I.; Sengupta, S. Imprints of the Janis-Newman-Winicour spacetime on observations related to shadow and accretion. *Phys. Rev. D* **2020**, *102*, 064027. [CrossRef]
37. Shaikh, R.; Banerjee, P.; Paul, S.; Sarkar, T. A novel gravitational lensing feature by wormholes. *Phys. Lett. B* **2019**, *789*, 270. [CrossRef]
38. Shaikh, R.; Banerjee, P.; Paul, S.; Sarkar, T. Strong gravitational lensing by wormholes. *JCAP* **2019**, *7*, 028. [CrossRef]